REPORT DOCUMENTATION PAGE

Form Approved
OMB NO. 0704-0188

1. AGENCY USE ONLY (Leave Blank)	2. REPORT DATE	3. REPORT TYPE AND DATES COVERED
	11/26/2006	Final report, July 3 2001 - October 2 2006

4. TITLE AND SUBTITLE

High-Performance Substrates for SERS Detection via Microphotonic Photopolymer Characterization and Coating with Functionalized Hydrogels

5. FUNDING NUMBERS

DAAD19-02-1-0287

6. AUTHOR(S)

Orlin D. Velev

7. PERFORMING ORGANIZATION NAME(S) AND ADDRESS(ES)

North Carolina State University
Raleigh, North Carolina, 27695

8. PERFORMING ORGANIZATION REPORT NUMBER

9. SPONSORING / MONITORING AGENCY NAME(S) AND ADDRESS(ES)

U. S. Army Research Office
P.O. Box 12211
Research Triangle Park, NC 27709-2211

10. SPONSORING / MONITORING AGENCY REPORT NUMBER

44022.1-CH

11. SUPPLEMENTARY NOTES

The views, opinions and/or findings contained in this report are those of the author(s) and should not be construed as an official Department of the Army position, policy or decision, unless so designated by other documentation.

12 a. DISTRIBUTION / AVAILABILITY STATEMENT

Approved for public release; distribution unlimited.

12 b. DISTRIBUTION CODE

13. ABSTRACT (Maximum 200 words)

The goal of this research project in collaboration with ARL-Edgewood was to design, characterize and fabricate a new generation of stable and highly enhancing SERS substrates for sensors with continuous detection of chemical agents in water streams. We completed a detailed systematic study of hierarchically templated SERS substrates in thin films. In this task, convective assembly at high volume fractions was used to assemble gold nanoparticles into structured porous films templated by colloidal crystals. The control over the film structure allowed optimizing their performance for potential sensor applications. The primary focus of the second newer research direction was the fabrication of nanostructured gold substrates in the form of millimeter and sub-millimeter dots for on-chip assays. The know-how gained from completion of previous research goals was used to fabricate SERS micropatches in small volumes with controlled micro and nanostructure for highly selective, high sensitivity assays. The process was modeled and a procedure for fabricating SERS microassay patches was formulated. The technique developed allows us to create in the next stages of our research a new generation of miniature arrays of SERS-based sensors.

14. SUBJECT TERMS

Chemical sensors, SERS substrates, microfluidic sensors, nanostructured materials

15. NUMBER OF PAGES

21

16. PRICE CODE

17. SECURITY CLASSIFICATION OR REPORT	18. SECURITY CLASSIFICATION ON THIS PAGE	19. SECURITY CLASSIFICATION OF ABSTRACT	20. LIMITATION OF ABSTRACT
UNCLASSIFIED	**UNCLASSIFIED**	**UNCLASSIFIED**	**UL**

REPORT DOCUMENTATION PAGE (SF298)
(Continuation Sheet)

Final Research Report to the Army Research Office

High-Performance Substrates for SERS Detection via Microphotonic Photopolymer Characterization and Coating with Functionalized Hydrogels

Principal Investigator: Orlin D. Velev

Institution: Department of Chemical and Biomolecular Engineering
North Carolina State University, Raleigh, NC 27695

Extended abstract. The goal of this research project in collaboration with ARL-Edgewood was to design, characterize and fabricate a new generation of stable and highly enhancing SERS substrates for sensors with continuous detection of chemical agents in water streams. We completed a detailed systematic study of hierarchically templated SERS substrates in thin films. In this task, convective assembly at high volume fractions was used to assemble gold nanoparticles into structured porous films templated by colloidal crystals. These hierarchically porous gold nanofilms were proven to be stable and efficient substrates for surface-enhanced Raman spectroscopy (SERS). The control over the film structure allowed optimizing their performance for potential sensor applications. We showed that both the nanoscale porosity and the long-range sub-micrometer ordering augment the signal intensity. The primary focus of the second newer research direction was the fabrication of nanostructured gold substrates in the form of millimeter and sub-millimeter dots for on-chip assays. The know-how gained from completion of previous research goals was used to fabricate SERS micropatches in small volumes with controlled micro and nanostructure for highly selective, high sensitivity assays. We proved the feasibility of the technique and characterized the parameters involved in the self-assembly process. The process was modeled and a procedure for fabricating SERS microassay patches was formulated. The technique developed allows us to create in the next stages of our research a new generation of miniature arrays of SERS-based sensors.

SUMMARY OF SCIENTIFIC RESULTS

Research papers resulting from this project

- D. M. Kuncicky and O. D. Velev, to be submitted to *Langmuir,* in preparation (2007). Engineered assembly of uniform hierarchically porous patches from colloid crystals inside sessile droplets.

- D. M. Kuncicky, K. Bose, K. D. Costa and O. D. Velev, *Chem. Mater.,* in press (2007). Sessile droplet templating of miniature porous hemispheres from colloid crystals.

- D. M. Kuncicky, B. G. Prevo and O. D. Velev, *J. Mater. Chem.,* **16**, 1207-1211 (2006). Controlled assembly of SERS substrates templated by colloidal crystal films.

- D. M. Kuncicky, S. D. Christesen and O. D. Velev, *Appl. Spectr.*, **59**, 401-409 (2005). Role of the micro- and nanostructure in the performance of SERS substrates assembled from gold nanoparticles.

- B. G. Prevo, Y. Hwang and O. D. Velev, *Chem. Mater.*, **17**, 3642-3651 (2005). Convective assembly of antireflective silica coatings with controlled thickness and refractive index.

- B. G. Prevo, J. C. Fuller, III and O. D. Velev, *Chem. Mater.*, **17**, 28-35 (2005). Rapid deposition of gold nanoparticle films with controlled thickness and structure by convective assembly.

- D. M. Kuncicky, S. D. Christesen and O. D. Velev, *Proc. SPIE Int. Soc. Opt. Eng.*, **5585,** 33-45, (2004). Engineering of SERS substrate structure: Role of micro- and nanoporosity.

Scientific presentations resulting from this project

- D. M. Kuncicky, O. D. Velev. "Engineered Assembly of Uniform Hierarchically Porous Patches from Metal Nanoparticles", AIChE Annual Meeting, San Francisco, CA, USA (November 2006, oral).

- D. M. Kuncicky, S. D. Christesen, O. D. Velev. "Engineering Hierarchically Porous Nanoparticle Patches for SERS Substrates", ACS Colloid and Surface Science Symposium, Boulder, CO, USA (June 21, 2006, oral).

- D. M. Kuncicky, S. D. Christesen, O. D. Velev. "Engineering Hierarchically Porous Films and Patches for SERS Substrates", MRS Fall Meeting, Boston, MA, USA (Nov. 29, 2005, poster).

- D.M. Kuncicky and O.D. Velev. "Fabricating SERS substrates in thin films and sessile droplets", Surfactants and Colloids Workshop, University of Hull, England (May, 2005, oral).

- D. M. Kuncicky, S. D. Christesen, O. D. Velev. "Engineering of SERS Substrate Structure: Role of Micro- and Nanoporosity", SPIE International Symposium Optics East, Philadelphia, PA, USA (October, 26, 2004, oral).

- D. M. Kuncicky, S. D. Christesen, O. D. Velev. "Role of the Micro- and Nanostructure in the Performance of SERS Substrates Assembled from Gold Nanoparticles", ACS PRF Summer School on Nanoparticle Materials, Ypsilanti, MI, USA (June, 7, 2004, poster).

- D. Kuncicky, P. M. Tessier, S. D. Christesen, O. D. Velev, "Surface-Enhanced Raman Spectroscopy Sensors Based on Gold Nanostructured Films Templated by Colloidal Crystals", Joint Service Scientific Conference on Chemical and Biological Defense, Towson, MD, USA (Nov. 17, 2003, oral).

- B. G. Prevo, J. C. Fuller, O. D. Velev, "Rapid deposition of gold nanoparticle films with controlled thickness and structure by convective assembly", MRS Spring Meeting, San Francisco, CA, (April 2003, poster).

- O.D. Velev, "Controlled assembly of materials and devices from nanoparticles, microparticles and live cells", Sandia National Laboratory, Albuquerque, NM, (May 2005, invited seminar).

- B. G. Prevo, Y. Hwang and O. D. Velev, "Controlled deposition and modification of conductive and antireflective nanoparticle coatings", 79th ACS Colloid and Surface Science Symposium, Potsdam, NY (June 2005, oral).

- D. M. Kuncicky, S. D. Christesen, O. D. Velev, "Engineering of SERS substrate structure for chemical sensors: Role of micro- and nanoporosity", ACS National Spring Meeting, San Diego, CA (March 2005, oral).

- O. D. Velev et al., "Tools for fast and controllable fabrication of photonic structures via particle self-assembly", MRS Fall Meeting, Boston, MA, (December 2003, invited).

- O. D. Velev et al., "Templated assembly of composite materials with photonic and electronic functionality", 2003 Composites at Lake Louise Meeting, Lake Louise, Canada (October 2003, invited, keynote).

- O. D. Velev, "Fast and controllable fabrication of photonic structures via particle self-assembly", NSF Workshop on Fundamental Research Needs in Photonic Materials Synthesis and Processing at the Interface, Rochester, NY, (April 2003, invited).

- O. D. Velev, "Rapid and controllable fabrication of photonic and electronic structures via particle self-assembly", Army Research Laboratory (ARL), Maryland, December 2003 (invited seminar).

- O. D. Velev, "Novel tools for rapid controlled assembly of nanoparticles, microparticles and droplets", Air Force Research Laboratory (AFRL), Denton, OH, (July 2003, invited seminar).

Research results and deliverables

Research goal 1: Controlled assembly of SERS substrates templated by colloidal crystal films

We used convective assembly to deposit films from chemically unmodified metallic nanoparticles on plain nonfunctionalized glass substrates.[1,2] We developed a procedure for concentrating of the nanoparticles by membrane filtration via centrifugation, and an apparatus for convective assembly at high volume fractions (Figure 1) that allows efficient rapid deposition of nanocoatings.[3-5] The combination of these two techniques allowed controlled and efficient assembly of a wide variety of thin structures from as-synthesized gold nanoparticles. The data obtained was used to engineer the structure of such self-assembled substrates in order to optimize their performance in realistic sensor applications with SERS-based signal transduction.

Templating metallic nanoparticles into "inverse opal" films

The apparatus for convective assembly that we developed requires only microliters of suspension and less than an hour of deposition time without the need for any complex or costly equipment. The particles dispersed in the liquid are transported to the edge of the growing crystal by the flux of the liquid compensating for evaporation from the crystal surface (Figure 1). This process, referred to as "convective assembly" or "evaporation induced self assembly," takes place near the meniscus of evaporating liquid films.[6-8] The particles concentrated and confined in the thin film are ordered into a colloidal crystal by reduction of free

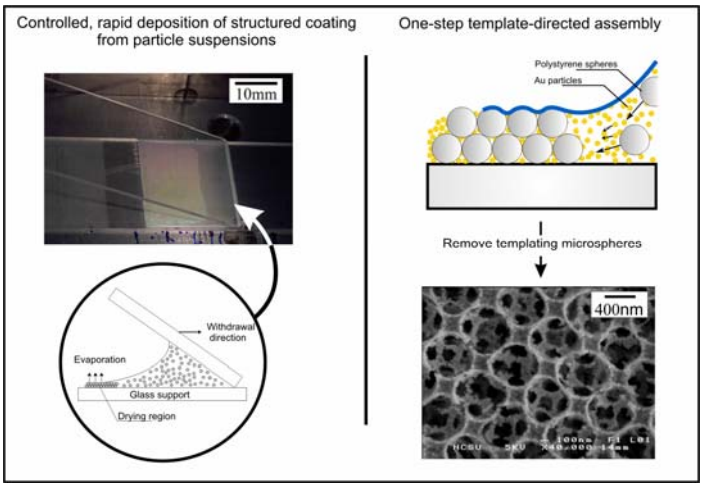

Figure 1. Schematic of the experimental setup for colloidal crystal assembly (left), and one-step template directed fabrication of SERS substrates (right). The order–disorder transition between the meniscus and the iridescent deposited crystal is clearly visible in the upper left image showing the actual process of deposition of a colloidal crystal coating.

volume and capillary immersion forces.[9] The mechanism is similar to the popularized "coffee ring" effect.[10,11] For thin films of spherical particles, the predominant microstructure formed is hexagonal close-packed crystals with (111) plane oriented parallel to the substrate. These films are typically polycrystalline due to multiple nucleation sites along the drying region. Arrays with square ordering are seen locally, but they appear to be a transition phase between the more stable hexagonally packed regions.[3] In the confined geometry of the thin films there is a competition between the thermodynamically favored packing density and the film thickness available to the particles layers. Square arrays are the thermodynamically preferred organization in layers of certain thickness,[12] however it is rarely observed in films deposited from latex spheres. This is likely due to the flexibility of the liquid/air interface, which permits particle protrusion through the liquid meniscus, hence allowing the formation of the hexagonal, rather than square, arrays.[3]

The method could be adapted for a single step fabrication of templated metallic nanostructures via convective assembly of a binary mixture of sacrificial microspheres and metallic nanoparticles (Figure 1). This is the basis of our procedure for fabricating SERS substrates. Small Au nanoparticles (10 - 20 nm) added to the suspension infiltrate the interstitial space surrounding the larger sacrificial microspheres (400 - 1000 nm). The aggregated nanoparticles replicate the microstructure imparted by the larger aggregated spheres. The templating spheres can be removed after deposition to yield an "inverse opal" metal film of defined thickness (Figure 1). The presence of the concentrated nanoparticles during the convective assembly process assists the formation of microsphere crystals with square packing symmetry. This type of lattice likely results from the reduced mobility (geometric confinement) of the larger microspheres in drying films of mixed concentrated particles.

Probing the structure-dependent SERS performance of the templated metallic films

The template-directed convective assembly technique allows for tuning the porosity on two hierarchical length scales. Microstructured cavities remain after removing the sacrificial template, and smaller nanopores are formed in between the gold particles. The size of these features can by controlled by varying the size of latex beads and the gold

nanoparticles used during assembly. The type, quality and structure of the template colloidal crystal depend primarily on the withdrawal speed and volume fraction of the colloidal suspensions used in the process.[1-3] By varying these parameters we fabricated latex templates that were polycrystalline with single crystal dimensions in the 5–20 μm range, or randomly packed with no apparent long-range crystal order (Figure 2). As a control, gold nanoparticle films were also prepared without using latex templating. All experimental measurements were performed using a point sampling protocol in a microfluidic flow cell.[13,14] Such online flow cells could be directly used as a basis for SERS sensors for continuous monitoring of water or gas fluxes. A matrix of experiments was designed to isolate individual contributions to the Raman enhancement arising from the nano- and microstructure. We collected multiple data points from randomly chosen spots on each SERS substrate inside the microfluidic chamber filled with liquid. This simulates application in real sensors where no drying and alignment to find "hot spots" is usually possible. Statistical analysis of the data was performed to determine the sensitivity of the substrates, and reproducibility of the fabrication technique. Such a statistical analysis is critical in evaluating the true performance characteristics of the SERS substrates. The porous gold substrates had a limit of detection of 150 ppb for sodium cyanide in water based on a five percent probability of false alarm.[13] Furthermore, the substrates performed well over a broad range of concentrations and pH values.[14]

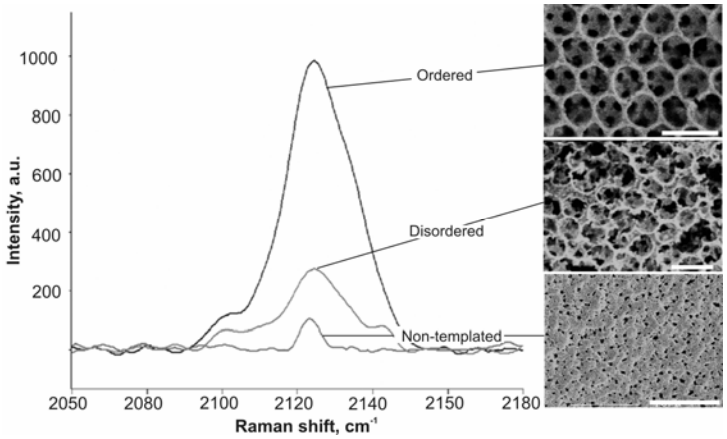

Figure 2. Effect of substrate structure on the SERS ignal intensity. Characteristic sodium cyanide spectra and SEM images collected in the continuous sampling microfluidic flow cell for ordered latex-templated (top), disordered latex-templated (middle), and non-templated (bottom) SERS substrates. Scale bars are 1 μm (top and middle micrographs) and 10 μm (bottom micrograph).[1]

The most intense SERS signals were reproducibly obtained on films with ordered polycrystalline micropores similar to the ones shown in Figure 2. We observed a multifold increase in intensity of the 2125 cm^{-1} peak for cyanide adsorbed on

the ordered crystalline regions compared with the disordered regions. The substrates without any templating were weakly enhancing, with a signal up to an order of magnitude lower than the microsphere templated ones. The variability of the peak intensity for the templated substrates (both ordered and disordered) was ca. 20% compared with ca. 75% for the non-templated example.[13] One of the major reasons SERS is not a widely used technology is the lack of standardized substrates that have uniform and reproducible SERS performance on any equipment. Poor reproducibility and hence high false alarm rates can be a fatal flaw for any routine diagnostic technique. These results demonstrate that the engineered templated deposition could produce substrates with consistently high signals, and may be an effective route to make substrates for SERS-based sensors for practical chemical analysis.

The convective assembly method also allows characterization of the effect of substrate thickness by depositing films with controlled numbers of nanoparticle layers. These experiments, however, were performed with non-templated films, as the structure of the colloidal crystals varies with the number of layers.[3] We found that the nanoparticle film thickness has little effect on SERS signal intensity for substrates thicker than a monolayer. This finding probably reflects the fact that only the particles in the top layer are illuminated by the excitation laser and hence contribute to the SERS signal. The practical significance is that only a relatively thin layer of gold nanoparticles is required to generate a strong signal.

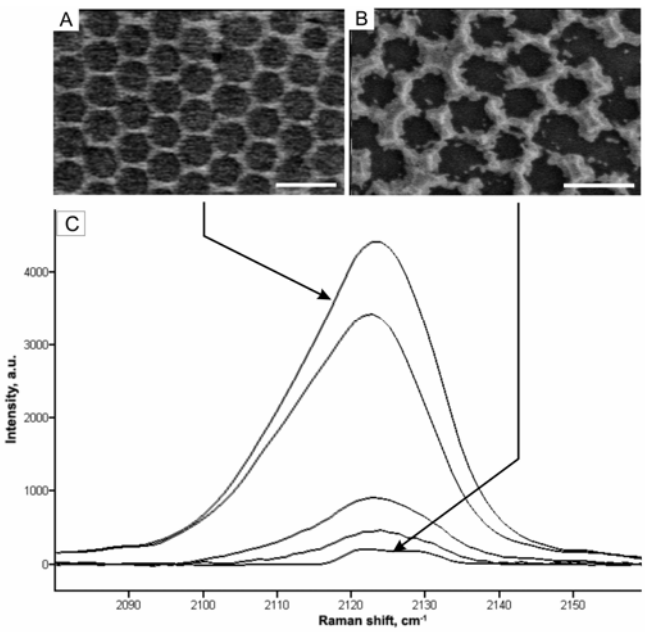

Figure 3. Effect of the substrate nanoporosity on SERS spectra intensity. SEM images collected from the (A) non-fused and (B) fused regions of the substrate with a nanoporosity gradient. Scale bars = 1 μm. (C) Raman spectra collected sequentially moving from the non-fused end (top spectra) to the highly-fused end (bottom spectra).[1]

Finally we characterized the effect of the nanoporosity inherent in the aggregated structure of touching particles (Figure 3). The nanoporosity

can be changed by controlled post-deposition fusion of the gold nanoparticles at temperatures between 200 and 500 ^{o}C. In order to reliably characterize the effect of the nanoporosity on SERS performance we developed a procedure for making nanoporosity gradient substrates by imposing a monotonically varying thermal gradient onto the backside of the SERS support.[1] This technique produced substrates that had fully fused gold nanoparticles on one end and unchanged discreet aggregated gold nanoparticles on the other, with a variable degree of fusion in the middle. The degree of nanoporosity along the sample surface after heating could be correlated to the spatially varying color change of the gold nanocoating. The substrate retained its characteristic reddish brown color on the non-fused side and gradually took on a golden color towards the fully fused end. The formation of large continuous metal domains from fused particles was evidenced by the extreme broadening of the surface plasmon resonance (SPR) adsorption peak centered on 780 nm.

Examination of the heat-treated end of substrates with SEM verified that the microscale pores left over from latex templates were retained throughout the entire film structure (Figure 3). The SERS signal was highest for the unheated region, and decreased commensurate with the degree of particle fusing (Figure 3). These data convincingly demonstrate that nanoscale surface roughness stemming from the discrete aggregated gold particles is a key factor directly related to high SERS performance. While it may be expected that nanoscale roughness generates stronger plasmon resonances, this may not be the only major effect here. Our working hypothesis is that the strong SERS response collected from the nanoporous substrates is closely related to the large surface area which allows more cyanide to adsorb from the surrounding solution.

In addition to the direct structure engineering experiments we also performed a cycle of experiments where we fabricated new substrate architectures using anisotropic Au nanoparticles and size-tailored micropores to promote ultrasensitive detection and optimized protein adsorption. We made progress towards the evaluation of the feasibility of using our templated Au substrates with a newly reported Raman based signal transduction for bioassays. Procedures for surface functionalization of the gold substrates with Dithiobis(succinimidyl-2-nitrobenzoate (DSNB) that contains a strongly

scattering nitro group and can be used as a reporter label in bioassays were developed in collaboration with the group of Prof. S. Franzen at NCSU.

Thin film SERS substrates: Concluding remarks

The cycle of experiments perfomed in this project proves that while both the micro- and the nanostructure contribute to the high enhancement of our substrates it is the nanopores that lead to the key effect. The presence of sub-micron pores left behind by the sacrificial latex beads and the long-range ordering of these large pores also contribute to the enhancement of these substrates. Less than a milligram of nanoparticles is required to coat a surface of tens of square millimeters. The gold substrates were proven to be highly stable and to have a shelf life of at least a year. Since they are made from inert gold, the problem of physical and chemical deterioration common to silver-based SERS substrates is avoided. These substrates can serve as a basis for biomolecular detection in solution.

Research Goal 2 - Deposition of arrays of SERS-active micropatches from evaporating droplets.

The second major research thrust has been the development of nanostructured gold substrates in the form of millimeter and sub-millimeter dots for SERS sensing. The most common SERS substrates made by us or others are in the form of patches and stripes of size from millimeters to centimeters. There are a range of important advantages that can be derived from making SERS-active micropatches. For one, this would allow further miniaturization, use of microfluidic chambers and samples which can have volumes as small as a few picoliters.[15,16] In the longer perspective, this can open new areas of research, where chips of arrays of microdots of different functionality can be interrogated by SERS, thus making an analogue of the presently used parallel bioassays, but with drastically improved function and sensitivity. The fundamentals of drying of suspension droplets onto substrates could also benefit other areas of research and technology, such as

the fabrication of DNA microassays by inkjet printing and porous microindenters for biomechanical studies of whole cells and biological surfaces.

The simplest approach to depositing gold nanoparticles and latex template spheres in small spots would be to dry droplets of suspension on a substrate. If metallic nanoparticles are added to the droplet, latex crystal - gold nanoparticle patches of round flat shape, equivalent in structure to the SERS material precursors could be formed. This process, however, usually does not yield well-shaped patches, but instead forms a "coffee rings" as the particles are concentrated at the droplet periphery. The formation of uniform and well-structured particle assemblies from sessile droplets thus requires intricate control over the drying dynamics of the droplet, and the resulting process of particle assembly.

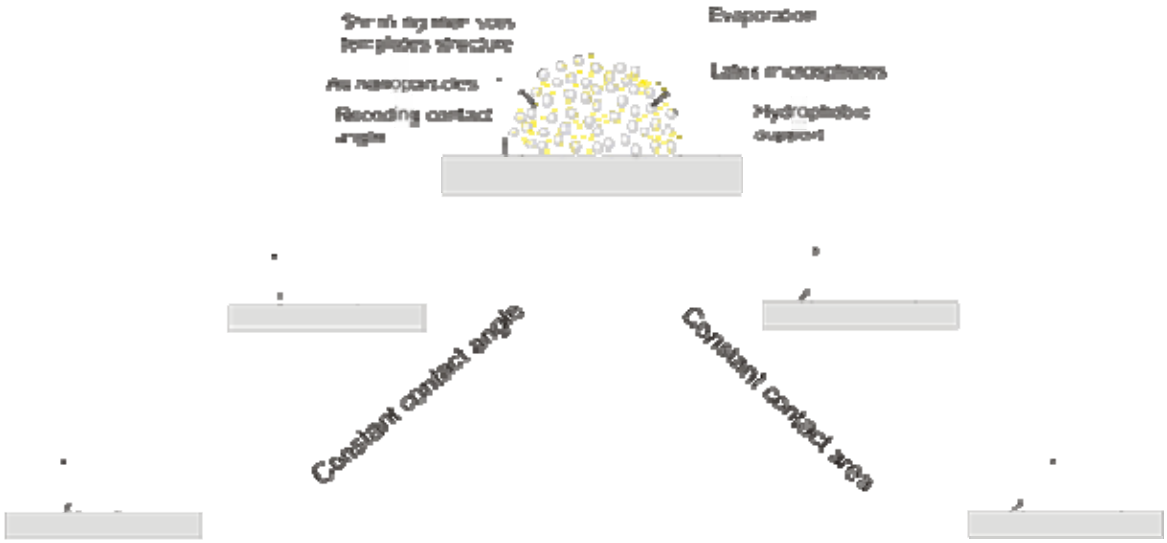

Figure 4. Schematic of the two ideal modes of evaporation showing the process of meniscus templating in sessile droplets.

The first goal was to characterize in detail the role of the contact angle, the droplet volume, particle volume fraction, and addition of electrolyte on the size and shape of the patches assembled during the drying process. This was done by a combination of experiment and modeling of the mass-transfer process. We developed an experimental methodology for precise, repeatable patch deposition. The characterization of the process

in detail allowed us to optimize the deposition conditions and formulate protocols for deposition of nanostructured patches of different diameter, thickness and functionality.

In-depth experimental and theoretical characterization of the pocess of colloidal templating in sessile droplets

The shape of the templating meniscus and the dynamics of the receding contact line are critical elements in the micropatch formation process. The droplets could dry at constant contact angle with decreasing contact area, or constant contact area with decreasing contact angle (Fig. 4).[17-20] For real liquids, the mode of evaporation, and hence, the profile change also depends on droplet volume,[21, 22] evaporation rate,[23] substrate roughness, and substrate chemical heterogeneity.[24-26] Drying of droplets from particle suspensions introduces an additional set of complexities. Particle-surface interactions, particle-particle interactions, and convective particle motion within the drying drop can influence meniscus shape and kinetics of sessile droplet evaporation.[27-33] Here we summarize the parameters used to describe the shape of the meniscus and the basics of drying droplets dynamics in the diffusion limited regime that were used to interpret the data. The small volumes used allowed us to neglect gravitational forces when estimating the meniscus shape during drying. The templating meniscus shape is determined by the balance of the surface tension force and gravitational force exerted on the drop. The ratio of these forces is expressed by the dimensionless Bond number, $Bo = \rho g R^2/\gamma$ where ρ is the density of water, g is the acceleration due to gravity, R the droplet radius of curvature and γ is the surface tension of water. For the droplet volumes studied here $Bo \sim 10^{-1}$. Thereby, to a good approximation meniscus geometry is a spherical cap, although some flattening may occur, but likely with marginal significance in data interpretation when compared to other sources of error in the experiments. The accuracy of the spherical cap approximation is tested by calculating a circularity value for the droplets. This is done by taking the ratio of measured cross-sectional area to spherical cap cross sectional area fit by Equation 1 where a is contact radius and h droplet height. A circularity of one corresponds to a spherical cap, and the value decreases commensurate with increased flattening of the droplet.

$$A_{segment} = \frac{4}{3}ah + \frac{1}{4}\frac{h^3}{a} \tag{1}$$

The 4 μL droplets studied experimentally have a circularity value of 0.99 indicating little deformation of the cap due to gravity. The spherical geometry is practically significant since the position of the air-liquid boundary is specified by only two of the measured variables. Thereby, droplet volume, V, and surface area, S, are easily calculated (Eqns. 2, 3) and related to the mean evaporative flux, N_e (Eqn. 4).

$$V = \frac{1}{6}\pi h\left[3a^2 + h^2\right] = \frac{1}{3}\pi R^3 E \tag{2}$$

$$E = 2 - 3\cos\theta + \cos^3\theta$$

$$S = \pi(a^2 + h^2) = 2\pi R^2(1 - \cos\theta) \tag{3}$$

$$N_e = -\rho\frac{1}{S}\frac{dV}{dt} \tag{4}$$

For diffusion controlled evaporation without particles, a good fit between theory and experiment is obtained with a straightforward macroscopic material balance (Eqn. 4.), and the assumption that the vapour concentration distribution satisfies the Laplace equation (Eqn. 5). After applying boundary conditions to solve for N_e, equation 6 is obtained. The dynamic change in volume is related to the water vapour in air diffusivity, D, and the difference between water vapour concentration at the surface, C_s, and of the ambient air in the room, C_∞. C_s and C_∞ are related to the vapour pressure of water, P_{vapor}, through the ideal gas law and the relative humidity, H, as shown by Eqn. 5 where R is the universal gas constant and T the room temperature.

$$\frac{d}{dr}\left(r^2\frac{dC}{dr}\right) = 0 \qquad C_s(r = R) = \frac{P_{vapor}}{RT};\, C(r \to \infty) = C_\infty \tag{5}$$

$$\frac{dV}{dt} = -\frac{4\pi D}{\rho}R(C_s - C_\infty) \tag{6}$$

Extending this result to sessile droplets requires a geometrical factor, $A(\theta)$ which accounts for the reduced volume available for evaporation due to the substrate. Using Eqn. 2 the following relationship is obtained.

$$\frac{d}{dt}V^{2/3} = -8\left(\frac{\pi}{3}\right)^{2/3} K \frac{A(\theta)}{E^{1/3}}$$

$$A(\theta) \to 0, \theta \to 0; A(\theta) = 0.5, \theta = \pi/2; A(\theta) = \ln(2), \theta = \pi \qquad (7)$$

$$K = \frac{D(C_s - C_\infty)}{\rho}$$

Equation 7 shows that the dynamics are quite different between the cases of drying at constant contact angle versus constant contact area. Since $A(\theta)$ is constant for a fixed contact angle, the analytical solution for $V(t)$ shows a linear $V^{2/3} - t$ decay. On the other hand, when the contact area is fixed, $A(\theta)$ diminishes concomitant with decreasing contact angle, and no simple analytical solution exists. However, for a broad range of contact angles, the air-liquid surface area changes little for droplets drying in this regime. As a consequence dV/dt has a weak time dependence, and changes little over the droplet lifetime.[17, 19] The simple macroscopic model presented is used as a basis for comparison with the experimental results and data interpretation.

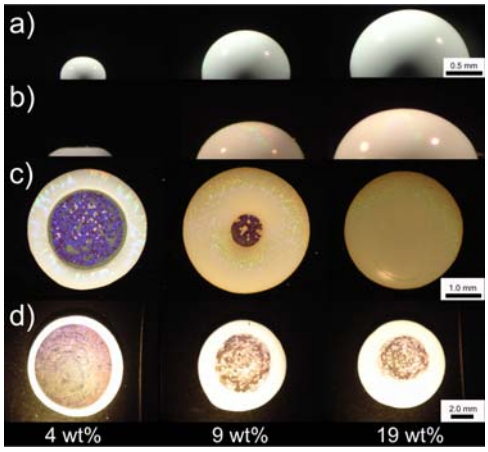

Figure 5. Micrographs of dried micropatches of typical results of sessile droplet templating experiments showing the effect of particle concentration and contact angle. The micropatches shown in a) – d) were deposited on substrates of contact angle 101°, 80°, 50°, and vanishing one.

The theoretical description of drying colloidal suspension droplets is more complicated. Hydrodynamic effects, sedimentation, particle aggregation, and particle-substrate sticking can exert a pronounced influence on the particle assembly process inside the drying drop. When the contact line is pinned spatially varying evaporation

drives solvent towards the three-phase contact line were the evaporation rate is highest.[29, 30] This effect is especially pronounced for low contact angles and strongly pinned contact lines. When possible the experiments were designed to limit the number of such variables that drive formation of non-uniform micropatch assemblies. A suitable microsphere diameter, a, was determined by gauging the relative importance of the thermodynamic versus gravitational forces using the Peclet number for sedimentation.[33] Here $\Delta\rho = (1055 - 998)$ kg m^{-3} is the density difference between water medium and latex microsphere, g the acceleration due to gravity, k the Boltzmann's constant, and T the temperature. For 600 nm PS spheres $Pe \sim 10^2$, and there should be little settling during the one hour experiments. Importantly this size microspheres also yields the optimal porosity for the hierarchically templated SERS patches since the cavity diameter is comparable to the wavelength of the Raman laser excitation source.[1]

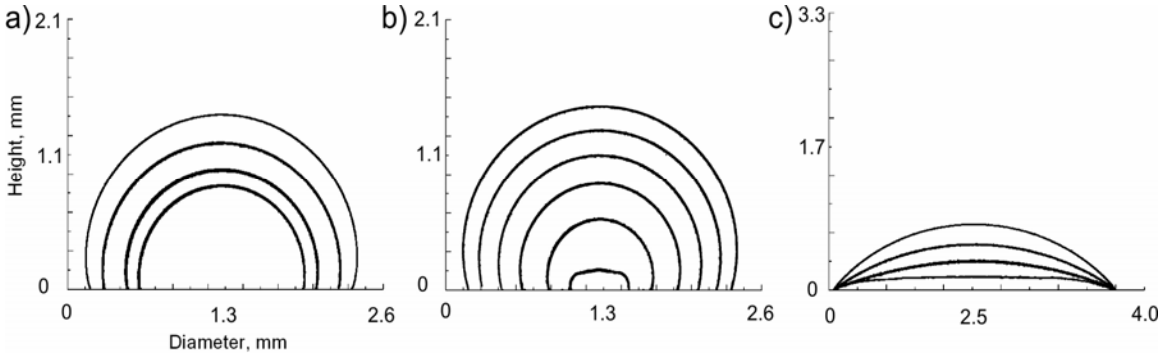

Figure 6. Drying droplet profile determined from side profile digital images taken at ten minute intervals. The parameters for each case are as follows: a) 4 μL drop containing 16 vol% microspheres deposited on a hydrophobic surface with 101° contact angle. b) 4 μL drop, 0.25 vol% microspheres, and 101° contact angle. c) 4 μL drop, 7.0 vol% microspheres, and 50° contact angle. Experiments conducted at 40%RH and 22° C.

$$Pe = \frac{4\pi a^3 \Delta\rho g h}{3kT} \tag{8}$$

An additional effect has been observed for particle suspensions and polymer solutions with a gelation point. The reological properties change at the meniscus due to local increase in concentration. Ultimately a mechanical instability can form inducing buckling, warping and cracking of the templating meniscus.[27, 33]

Identifying the stages of micropatch formation

A major objective of the experiments reported herein was to characterize the micropatch architecture in terms of experimentally accessible parameters. We found that during drying of microliter droplets of suspension on moderately hydrophobic surfaces with contact angle between 50° – 100° the dynamic shape of the meniscus can be controlled exclusively by the contact angle and particle concentration (Fig. 5). This allows for tuning the microparticle assembly architecture and dimensions by judicious choice of solid substrate and droplet volume. These experiments allowed us to outline the conditions conducive to depositing micropatches of controlled geometry.

The use of substrates of controlled contact angle was a necessary, but not sufficient condition for maintaining the desired micropatch shape throughout drying. We observed that upon lowering particle concentration the dry micropatch not only necessarily decreased in size, but surprisingly changed form as well (Figs 5, 6). The droplets deposited from low concentration PS suspensions had a flattened or dimpled shape. The degree of flattening was quantified by calculating the circularity of the dried patch. For suspensions dried on moderately hydrophobic surfaces with contact angle 81° and 101° the patches were concave at medium to high volume fractions. The droplets dried on lower contact angles substrates transition to a flattened cap at higher volume fractions. The flattening of the patch was even more pronounced for $\theta \leq 50°$.

We found that for sessile droplets of colloidal PS microspheres the observed shape is strongly correlated to the mode of drying. To assess the range of possible drying modes in the experiments, edge profiles extracted from the digital images were used to measure the evolving shape of the templating meniscus during drying (Figure 6). The "coffee ring" structure dominated for droplets deposited onto surfaces with $\theta \leq 50°$ (Figs. 5c, 5d, 6c). The contact line pinned within just a few seconds after deposition. The particles were concentrated and confined in the thin film that formed and were transported to the periphery by the flux of liquid compensating for evaporation near the three-phase contact line. The drying dynamics turned out to be markedly different when droplets were deposited onto moderately hydrophobic surfaces (Figs 5a, 5b, 6a, 6b). During the first few minutes the contact line is pinned, and the contact angle concurrently

decreases. The degree of hysteresis is substrate dependent and increases for substrate with larger RMS roughness. The initial stage was followed by release of the contact line, and a prolonged period of drying with little change in contact angle. Eventually the contact line re-pinned. The re-pinning resulted in a droplet that deformed as particles were concentrated near the periphery. During this final stage the shape of the micropatch began to take form.

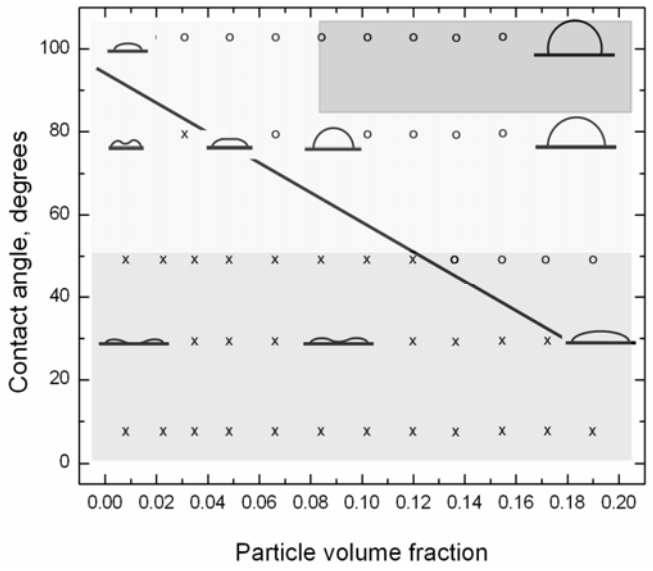

Figure 7. Categorized micropatch shape determined from optical micrographs and calculated circularity values. The drawn cross section profiles show how patch architecture varies with volume fraction and contact angle. The open circles(○) correspond to patches with parabolic shape and the crosses (×) to patches with dimpled or coffee ring shape. The line shows the edge transition corresponding to the most uniform and flat micropatches.

This series of observations are categorized in the phase diagram shown in Figure 7. This chart allows for *a priori* determination of patch architecture based on initial conditions of contact angle and particle volume fraction. Most importantly the line drawn highlights the transition from the parabolic shape to dimpled shape showing the correct conditions for producing flat uniformly shaped. These results provided the basis for controlled fabrication of the templated SERS microarray shown in Figure 8. They have a strong generality and their relevance to a broad range of colloidal and materials processes will be investigated in detail in the future.

Size–tailored micropores to promote ultrasensitive detection and optimized protein adsorption

Previously, we showed that the latex templated substrates have an enhancement on the order of 10^4. This may be sufficient for strongly chemisorbing species such as cyanide - an LOD of ca. 150 ppb has been demonstrated for sodium cyanide in water or molecules with large Raman cross sections. Non-polar molecules and biological macromolecules, however, are more problematic. In collaboration with Biopraxis, Inc. (San Diego, CA) we have worked towards optimizing the substrate structure for direct protein detection. A potential problem with SERS-based protein detection lies in intercalating the macromolecules within the active region of the SERS matrix. If the protein is too big to fit in the templated pores it is likely that the Raman signal will be weak.

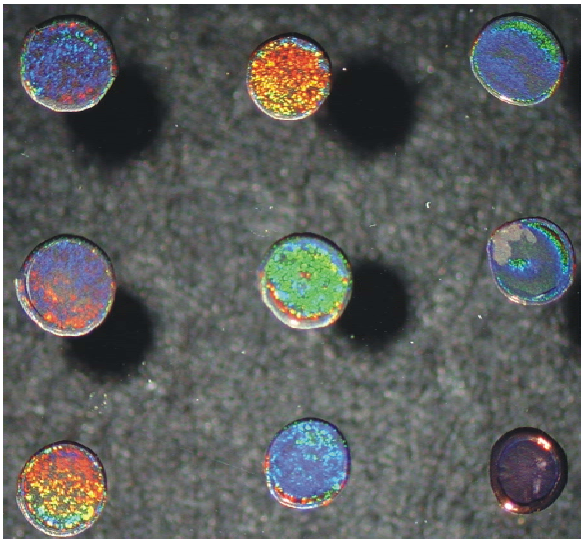

Figure 8. Arrayed micropatch SERS substrates. Each element in the array consist of 20 nm gold particles templated around latex spheres ranging in size from 400 nm to 1.1 μm.

A host of experiments were designed to isolate the chemical and structural parameters that contribute to and yield the highest Raman enhancement for protein binding. The sessile drop substrate fabrication method described above allowed for easily tuning the porosity on these two hierarchical length scales by simply varying the gold particle or template sphere size. This method allowed us to make an arrayed format SERS grid (Fig. 8) where each element consists of a different sized template or different sized gold particles. The analogous thin film SERS substrates with varied template and gold particle size have also been prepared. Efficient binding and intercalation of the protein into the SERS substrate must be achieved to yield large signals suitable for technologically relevant SERS-based assays. One potentially powerful functionalization approach we have explored was to take silica particles (which can be coated with biomolecules suitable for biospecific binding), and use them as template microspheres. Anisotropic gold particles are expected to yield additional Raman enhancement due to the

"lightning rod" effect. We have synthesized elliptical Au particles and successfully incorporated these particles into our SERS substrates. In summary, we have delivered a host of techniques that move SERS towards the use of repeatable, high-performance tuned and stable substrates. We have developed techniques for depositing these substrates in microfluidic chambers, making arrays of SERS micropatches and unding them in biomolecule detection.

References

1 D. M. Kuncicky, S. D. Christesen, and O. D. Velev, *Appl. Spectrosc.,* 2005, **59**, 401.

2 D. M. Kuncicky, B. G. Prevo, and O. D. Velev Kuncicky, D. M., Prevo, B. G., and Velev, O. D.; Controlled Assembly of SERS Substrates Templated by Colloidal Crystal Films, *J. Mat. Chem., 2006* **16**, 1207.

3 B. G. Prevo and O. D. Velev, *Langmuir,* 2004, **20**, 2099.

4 P. M. Tessier, O. D. Velev, A. T. Kalambur, J. F. Rabolt, A. M. Lenhoff, and E. W. Kaler, *J. Am. Chem. Soc.,* 2000, **122**, 9554.

5 P. Tessier, O. D. Velev, A. T. Kalambur, A. M. Lenhoff, J. F. Rabolt, and E. W. Kaler, *Adv. Mater.,* 2001, **13**, 396.

6 P. Jiang, J. F. Bertone, K. S. Hwang, and V. L. Colvin, *Chem. Mater.,* 1999, **11**, 2132.

7 N. D. Denkov, O. D. Velev, P. A. Kralchevsky, I. B. Ivanov, H. Yoshimura, and K. Nagayama, *Langmuir,* 1992, **8**, 3183.

8 C. J. Brinker, Y. F. Lu, A. Sellinger, and H. Y. Fan, *Adv. Mater.,* 1999, **11**, 579.

9 P. A. Kralchevsky and N. D. Denkov, *Curr. Opin. Colloid Interface Sci.,* 2001, **6**, 383.

10 R. D. Deegan, O. Bakajin, T. F. Dupont, G. Huber, S. R. Nagel, and T. A. Witten, *Nature,* 1997, **389**, 827.

11 H. Hu and R. G. Larson, *J. Phys. Chem. B,* 2002, **106**, 1334.

12 B. Pansu, P. Pieranski, and L. Strzelecki, *J. Phys. Paris,* 1983, **44**, 531.

13 D. M. Kuncicky, S. D. Christesen, and O. D. Velev, *Proc. SPIE,* 2004, **5585**, 33.

14 P. M. Tessier, S. D. Christesen, K. K. Ong, E. M. Clemente, A. M. Lenhoff, E. W. Kaler, and O. D. Velev, *Appl. Spectrosc.,* 2002, **56**, 1524.

15 H. Y. Ko, J. Park, H. Shin, and J. Moon, *Chem. Mater.* 2004, **16**, 4212.

16 D. M. Kuncicky, K. Bose, K. D. Costa and O. D. Velev, *Chemistry of Materials,* (In Press).

17 Picknett, R. G.; Bexon, R. *J. Colloid Interface Sci.* **1977,** 61, 336-350.

18 Bourges-Monnier, C.; Shanahan, M. E. R., *Langmuir* **1995,** 11, 2820-2829.

19 Rowan, S. M.; Newton, M. I.; McHale, G. *J. Phys. Chem.* **1995,** 99, 13268-13271.

20 Erbil, H. Y.; McHale, G.; Newton, M. I. *Langmuir* **2002,** 18, 2636-2641.

21 Birdi, K. S.; Vu, D. T.; Winter, A. *J. Phys. Chem.* **1989,** 93, 3702-3703.

22 Fang, X. H.; Li, B. Q.; Petersen, E.; Ji, Y.; Sokolov, J. C.; Rafailovich, M. H. *J. Phys.Chem. B* **2005,** 109, 20554-20557.

23 Rowan, S. M.; McHale, G.; Newton, M. I.; Toorneman, M. *J. Phys. Chem. B* **1997,** 101, 1265-1267.

24 Degennes, P. G. *Rev. Mod. Phys.* **1985,** 57, 827-863.

25 Blossey, R. *Nat. Mater.* **2003,** 2, 301-306.

26 Soolaman, D. M.; Yu, H. Z. *J. Phys. Chem. B* **2005,** 109, 17967-17973.

27 Parisse, F.; Allain, C. *Langmuir* **1997,** 13, 3598-3602.

28 Tsapis, N.; Dufresne, E. R.; Sinha, S. S.; Riera, C. S.; Hutchinson, J. W.; Mahadevan, L.; Weitz, D. A. *Phys. Rev. Lett.* **2005,** 94, 018302.

29 Hu, H.; Larson, R. G. *J. Phys. Chem. B* **2006,** 110, 7090-7094.

30 Deegan, R. D. *Phys. Rev. E* **2000,** 61, 475-485.

31 Fischer, B. J. *Langmuir* **2002,** 18, 60-67.

32 Truskett, V.; Stebe, K. J. *Langmuir* **2003,** 19, 8271-8279.

33 Sugiyama, Y.; Larsen, R. J.; Kim, J. W.; Weitz, D. A., *Langmuir* **2006,** 22, 6024-6030.

34 W. B. Russel, D. A. Saville, and W. R. Schowalter, *Colloidal Dispersions*, Cambridge 1989.